UDC 621.3 https://doi.org/10.20998/2074-272X.2021.3.09

N. Belbachir, M. Zellagui, S. Settoul, C. Z. El-Bayeh, B. Bekkouche

# SIMULTANEOUS OPTIMAL INTEGRATION OF PHOTOVOLTAIC DISTRIBUTED GENERATION AND BATTERY ENERGY STORAGE SYSTEM IN ACTIVE DISTRIBUTION NETWORK USING CHAOTIC GREY WOLF OPTIMIZATION

***Goal.*** *The integration of photovoltaic distributed generations in the active distribution network has raised quickly due to their importance in delivering clean energy, hence, participating in solving various problems as climate change and pollution. Adding the battery energy storage systems would be considered as one of the best choices in giving solutions to the mentioned issues due to its characteristics of quick charging and discharging, managing the quality of power, and fulfilling the peak of energy demand.* ***The novelty*** *of the proposed work is the development of new multi-objective functions based on the sum of the three technical parameters of total active power loss, total voltage deviation, and total operation time of the overcurrent protection relay.* ***Purpose.*** *This paper is dedicated for solving the allocation problem of hybrid photovoltaic distributed generation and battery energy storage systems integration in the standard IEEE 33-bus and IEEE 69-bus active distribution networks.* ***Methodology.*** *The optimal integration of the hybrid systems is formulated as minimizing the proposed multi-objective functions by applying a newly developed metaheuristic technique based on various chaotic grey wolf optimization algorithms. The applied optimization algorithms are becoming increasingly popular due to their simplicity, lack of gradient information needed, ability to bypass local optima, and versatility in power system applications.* ***Results****. The simulation results of both test systems confirm the robustness and efficiency of the chaotic logistic grey wolf optimization algorithm compared to the rest of the algorithms in terms of convergence to the global optimal solution and in terms of providing the best and minimum multi-objective functions-based power losses, voltage deviation and relay operation time values.* ***Practical significance****. Recommendations have been developed for the use of optimal allocation of hybrid systems for practical industrial distribution power systems with the renewable energy sources presence.* References 32, tables 4, figures 9.

*Key words:* **photovoltaic distributed generation, battery energy storage system, active distribution network, optimal integration, multi-objective functions, chaotic grey wolf optimization algorithm.**

***Мета.*** *Інтеграція фотоелектричної розподіленої генерації в активну розподільчу мережу швидко зросла завдяки її важливості для доставки чистої енергії, отже, участі у вирішенні різних проблем, таких як зміна клімату та забруднення. Додавання акумуляторних систем накопичення енергії може бути розглянуто як один з найкращих варіантів вирішення зазначених питань завдяки своїм характеристикам швидкої зарядки та розрядки, управління якістю енергії та задоволення піку енергетичних потреб.* ***Новизна*** *запропонованої роботи полягає у розробці нових багатоцільових функцій на основі суми трьох технічних параметрів сумарних втрат активної потужності, загальних відхилень напруги та загального часу спрацьовування реле захисту від перевантаження по струму.* ***Мета.*** *Стаття присвячена вирішенню проблеми розподілу гібридних фотоелектричних розподілених систем генерації та інтеграції систем накопичення енергії в стандартні активні розподільчі мережі з 33-шинами IEEE та 69-шинами IEEE.* ***Методологія.*** *Оптимальна інтеграція гібридних систем сформульована як мінімізація запропонованих багатоцільових функцій шляхом застосування нещодавно розробленої метаевристичної методики, заснованої на різних хаотичних алгоритмах оптимізації сірого вовка. Застосовані алгоритми оптимізації стають дедалі популярнішими завдяки своїй простоті, відсутності необхідної інформації щодо градієнту, можливості обходу локальних оптимумів та універсальності в застосуваннях щодо енергосистеми.* ***Результати.*** *Результати моделювання обох тестових систем підтверджують надійність та ефективність хаотичного логістичного алгоритму оптимізації сірого вовка в порівнянні з іншими алгоритмами з точки зору збіжності до глобального оптимального розв'язання та з точки зору забезпечення найкращих і мінімальних багатоцільових функцій на основі втрат потужності, відхилення напруги та значень часу спрацювання реле.* ***Практичне значення.*** *Розроблено рекомендації щодо використання оптимального розподілу гібридних систем для реальних промислових розподільчих енергосистем із наявністю відновлюваних джерел енергії.* Бібл. 32, табл. 4, рис. 9.

*Ключові слова*: **фотоелектрична розподілена генерація, акумуляторна система накопичення енергії, активна розподільна мережа, оптимальна інтеграція, багатоцільові функції, хаотичний алгоритм оптимізації сірого вовка.**

**1. Introduction.** In the last years, the penetration of Renewable Energy Sources (RES) in the Active Distribution Network (ADN) has rapidly increased to address the problems of climate change and pollution. Photovoltaic Distributed Generation (PVDG) often uses ADN to access many RESs for their benefits in pollution reduction, voltage profile enhancement, and power loss reduction. However, large-scale PVDG sources in the ADN variations, on the other hand, may cause voltage fluctuations in power supply systems, resulting in a loss of the quality of power and some other issues that have sparked widespread concern. Additionally, increasing PV penetration in the future could pose a serious threat to the utility ADN reliability and stability.

The Battery Energy Storage Systems (BESS) has emerged as one of most successful solutions for dealing with these issues [1]. The BESS has become a popular method of smoothing active power variations of distribution grid connected PVDG sources at the common coupling point in recent years. The BESS enables quick charging and discharging, enhancing the versatility of ADN, especially those with multiple PVDG sources. In practice, the BESS provides ADN with a variety of services in several countries [2].

Recently, various researchers have been dedicated to develop an advanced solution that identifies the best locations and sizes for PVDGs and BESSs units to improve ADN operation and planning problems, as applying the Mixed Integer Linear Programming (MILP) to reduce the total cost of energy in ADN [3, 4], and MILP algorithm while considering the environmental and

economic aspects [5]. Stochastic Mixed Integer Linear Programming (SMILP) for overall network cost minimization with ADN reconfiguration [6], and the Mixed-Integer Second-Order Cone Program (MISOCP) to minimize real-time energy gap with uncertainties [7], and also using MISOCP to reduce the total cost's operation and BESS cost's investment considering soft open points of ADN [8]. Dynamic programming optimization algorithm to maximize the renewable DG consumption and BESS benefits [9]. Applying Genetic Algorithm (GA) for active power losses minimization [10], and applying GA for minimizing the BESS total cost, also the yearly cost of voltage-sag events [11], also GA for reducing the total net present value from BESS deployment over a specified planning horizon [12], and applied multi-player distributed optimization game algorithm to maximize the cost and benefits of BESS [13].

Applied Differential Evolutionary (DE) algorithm for minimizing the investment and maintenance costs considering time-varying load model [14]. Implantation of the Group Search Optimizer (GSO) algorithm to minimize the system stability index of ADN [15], Modified Bat Algorithm (MBA) for minimizing the system's total cost with various irradiances at different days [16], Hybrid Gravity Search Algorithm (HGSA) for reducing the BESS daily cost of maintenance and operation also its initial investment [17], used Teaching–Learning-Based Optimization (TLBO) algorithm for minimization of life cycle cost and gas emissions [18], Whale Optimization Algorithm (WOA) for reducing the ADN's power losses [19], Particle Swarm Optimization (PSO) algorithm for reducing the active power loss and the node voltages deviation indices with the dynamic hourly reconfiguration of ADN [20], Natural Aggregation Algorithm (NAA) for minimizing the investment and operation cost of the system, and the BESS's residual value [21], Harris Hawks Optimization (HHO) algorithm to minimize the sum of the bus voltage deviation and active power losses [22]. Recently in 2021, applied Simulated Annealing (SA) algorithm for utility profit maximization from energy arbitrage [23].

This paper has applied a new recent meta-heuristic which called the Grey Wolf Optimizer (GWO); an optimization algorithm inspired based on the hunting behavior of grey wolves that lives in wild nature [24]. The principal defies of GWO that it is easy to fall into the local optimum. Owing to the ergodicity of chaos, in this paper is included the theory of chaos into the GWO algorithm to strengthen its performance [25].

Practically, the operational objectives are conflicting in nature. Hence, the problem of allocating PVDG and BESS becomes a complex multi-objective function problem that optimizes multiple conflicting objectives. In this paper, an allocation problem of hybrid PVDG–BESS systems is formulated to minimize the Multi-Objective Functions (MOF) which can be solved by the various versions of Chaotic Grey Wolf Optimization (CGWO) algorithms.

**2. Mathematical problem formulation.**

**2.1. Multi-objective functions.** In this paper, aim to optimally locate and size the hybrid PVDG and BESS sources into ADN, by minimizing simultaneously the technical parameters of Total Active Power Loss (TAPL), Total Voltage Deviation (TVD), and Total Operation Time (TOT) of Non-Standard Overcurrent Relay (NS-OCR), which is based on new time-current-voltage tripping characteristic

$$MOF = Minimize \sum_{i=1}^{N_{bus}} \sum_{j=2}^{N_{bus}} \sum_{i=1}^{N_R} \left[ TAPL_{i,j} + TVD_j + TOT_i \right]. \quad (1)$$

Starting by, the TAPL of the distribution line, that can be expressed by [26, 27]

$$TAPL_{i,j} = \sum_{i=1}^{N_{bus}} \sum_{j=2}^{N_{bus}} APL_{i,j}, \quad (2)$$

$$APL_{i,j} = \alpha_{ij} \left( P_i P_j + Q_i Q_j \right) + \beta_{ij} \left( Q_i P_j + P_i Q_j \right), \quad (3)$$

$$\alpha_{ij} = \frac{R_{ij}}{V_i V_j} \cos\left( \delta_i - \delta_j \right), \quad (4)$$

$$\beta_{ij} = \frac{R_{ij}}{V_i V_j} \sin\left( \delta_i + \delta_j \right), \quad (5)$$

where $R_{ij}$ is the line resistance; $N_{bus}$ is the bus number; ($\delta_i$, $\delta_j$) and ($V_i$, $V_j$) are angles and voltages, respectively; ($P_i$, $P_j$) and ($Q_i$, $Q_j$) demonstrate active and reactive powers, respectively.

The second term is the TVD, which is defined as [28, 29]

$$TVD_j = \sum_{j=2}^{N_{bus}} \left| 1 - V_j \right|. \quad (6)$$

The final term, the TOT of NS-OCR, which is defined as [30]

$$TOT_i = \sum_{i=1}^{N_R} T_i, \quad (7)$$

$$T_i = \left( \frac{1}{e^{(1-V_{FM})}} \right)^K TDS_i \left( \frac{A}{M_i^B - 1} \right), \quad (8)$$

$$M_i = \frac{I_F}{I_P}, \quad (9)$$

where $T_i$ is the operation time of relay; $TDS$ is the time dial setting; $M$ is the multiple of pickup current and $V_{FM}$ represent the fault voltage magnitude; $I_F$ and $I_P$ represent the fault and the pickup current, respectively; $A$, $B$, and $K$ are the constants of relay, set to 0.14, 0.02, and 1.5, respectively; $N_R$ is the number of overcurrent relays.

**2.2. Equality constraints** can be expressed by the balanced powers equations

$$P_G + P_{PVDG} + P_{BESS} = P_D + APL, \quad (10)$$

$$Q_G = Q_D + RPL, \quad (11)$$

where ($Q_G$, $P_G$) represent the total reactive and active power from the generator; ($Q_D$, $P_D$) represent the total reactive and active power of the load; ($RPL$, $APL$) are the reactive and active power loss, respectively; $P_{PVDG}$ and $P_{BESS}$ are the output powers generated from PVDG and BESS, respectively.

**2.3. Distribution line constraints** would be given as inequality constraints

$$V_{\min} \le \left| V_i \right| \le V_{\max}, \quad (12)$$

$$\left| 1 - V_j \right| \le \Delta V_{\max}, \quad (13)$$

$$\left| S_{ij} \right| \le S_{\max}, \quad (14)$$

where $V_{\min}$, $V_{\max}$ are minimum and maximum of bus voltage limits; $\Delta V_{\max}$ is the maximum of voltage drop limits; $S_{ij}$ is the apparent power in the distribution line and $S_{\max}$ is the maximum of apparent power.

**2.4. PVDG-BESS units constraints** can be expressed as follow

$$P_{PVDG}^{\min} \le P_{PVDG} \le P_{PVDG}^{\max}, \quad (15)$$

$$P_{BESS}^{\min} \le P_{BESS} \le P_{BESS}^{\max}, \quad (16)$$

$$\sum_{i=1}^{N_{PVDG}} P_{PVDG}(i) \le \sum_{i=1}^{N_{bus}} P_D(i), \quad (17)$$

$$\sum_{i=1}^{N_{BESS}} P_{BESS}(i) \le \sum_{i=1}^{N_{bus}} P_D(i), \quad (18)$$

$$2 \le PVDG_{Position} \le N_{bus}, \quad (19)$$

$$2 \le BESS_{Position} \le N_{bus}, \quad (20)$$

$$N_{PVDG} \le N_{PVDG.\max}, \quad (21)$$

$$N_{BESS} \le N_{BESS.\max}, \quad (22)$$

$$n_{PVDG,i} / Location \le 1, \quad (23)$$

$$n_{BESS,i} / Location \le 1, \quad (24)$$

where $P_{PVDG}^{\min}$, $P_{BESS}^{\min}$ are the minimum of output power injected by PVDG and BESS, respectively; $P_{PVDG}^{\max}$, $P_{BESS}^{\max}$ are the maximum of output power injected by PVDG, and BESS, respectively; $N_{PVDG}$, $N_{BESS}$ are the PVDG and BESS units' number, respectively; $n_{BESS}$, $n_{PVDG}$ are the locations of PVDG and BESS units at bus $i$.

**3. Chaotic grey wolf optimization.** As long as the GWO algorithm could not always perform that well in identifying global optimal results, CGWO algorithm was developed basing on introducing chaos (chaotic maps) in GWO algorithm itself in order to improve its efficiency by generating random numbers.

**3.1. Grey wolf optimizer.** The GWO is an algorithm evolved by Mirjalili [24], basing on the inspiration from the leadership hierarchy behaviours and the grey wolves hunt mechanism in wild nature, where it begins the process of optimization by initiating a plant of candidate solutions randomly.

The three best candidate solutions in each iteration, are assumed as alpha, beta, and delta wolves, who take the lead toward to promising search space regions. The rest of grey wolves are considered as omega and need to encircle alpha, beta, and delta to find better solutions. The mathematical formulation of omega wolves is expressed as [24, 31].

Encircling prey: grey wolves encircle prey during the hunt. The mathematical model expressed as follows:

$$\vec{D} = \left| \vec{C}.\vec{X}_p(t) - \vec{X}(t) \right|, \quad (25)$$

$$\vec{X}(t+1) = \vec{X}_p(t) - \vec{A}.\vec{D}, \quad (26)$$

where $\vec{A}$ and $\vec{C}$ designate the coefficient vectors; $t$ designates the current iteration; $\vec{X}_p$ is the best solution's position vector obtained so far; $\vec{X}$ is the vector of position.

The vectors $\vec{A}$ and $\vec{C}$ can be calculated using these equations

$$\vec{A} = 2.\vec{a}.\vec{r} - \vec{a}, \quad (27)$$

$$\vec{C} = 2.\vec{r}, \quad (28)$$

where $a$ is the decreased linearly from 2 to 0 over the iterations course (in exploration and exploitation phases); $\vec{r}$ is the vector randomly initiated with uniform distribution between 0 and 1.

Hunting: in GWO, it is supposed that alpha ($\alpha$), beta ($\beta$), and gamma ($\delta$) have better knowledge about the prey's potential location, the three best solutions obtained firstly so far are saved and obligate the other search agents (including the omegas) to update their positions according to the best search agent's position

$$\vec{D}_\alpha = \left| \vec{C}_1.\vec{X}_\alpha - \vec{X} \right|, \quad (29)$$

$$\vec{D}_\beta = \left| \vec{C}_2.\vec{X}_\beta - \vec{X} \right|, \quad (30)$$

$$\vec{D}_\delta = \left| \vec{C}_3.\vec{X}_\delta - \vec{X} \right|, \quad (31)$$

$$\vec{X}_1 = \vec{X}_\alpha - \vec{A}_1.(\vec{D}_\alpha), \quad (32)$$

$$\vec{X}_2 = \vec{X}_\beta - \vec{A}_2.(\vec{D}_\beta), \quad (33)$$

$$\vec{X}_3 = \vec{X}_\delta - \vec{A}_3.(\vec{D}_\delta), \quad (34)$$

$$\vec{X}(t+1) = \frac{\vec{X}_1 + \vec{X}_2 + \vec{X}_3}{3}. \quad (35)$$

**3.2. Chaotic maps.** The various chaotic maps [32] used are represented by their mathematical equations:

*a. Chaotic Gauss:*

$$x_{k+1} = \begin{cases} 1 & x_k = 0 \\ \dfrac{1}{\mathrm{mod}(x_k, 1)} & otherwise \end{cases}. \quad (36)$$

*b. Chaotic Singer:*

$$x_{k+1} = 1.07\left(7.86x_k - 23.31x_k^2 + 28.75x_k^3 - 13.302875x_k^4\right). \quad (37)$$

*c. Chaotic Tent:*

$$x_{k+1} = \begin{cases} \dfrac{x_k}{0.7}, & x_k < 0.7 \\ \dfrac{10}{3}(1 - x_k), & x_k \ge 0.7 \end{cases}. \quad (38)$$

*d. Chaotic Sine:*

$$x_{k+1} = \frac{a}{4}\sin(\pi x_k), \quad a = 4. \quad (39)$$

*e. Chaotic Logistic:*

$$x_{k+1} = a x_k (1 - x_k), \quad a = 4. \quad (40)$$

**4. Simulation and analysis results.** The various algorithms were tested on the standards test system IEEE 33-bus and 69-bus ADNs represented in Fig. 1, which comprised active and reactive powers of 3715 kW and 2300 kVar for the first system, 3790 kW and 2690 kVar for the second system. Also, under a nominal voltage equal to 12.66 kV for both systems. Where every one of systems' buses, would be protected by a NS-OCR. In general, it is calculated 32 NS-OCRs for the first system and 68 NS-OCRs for the second system.

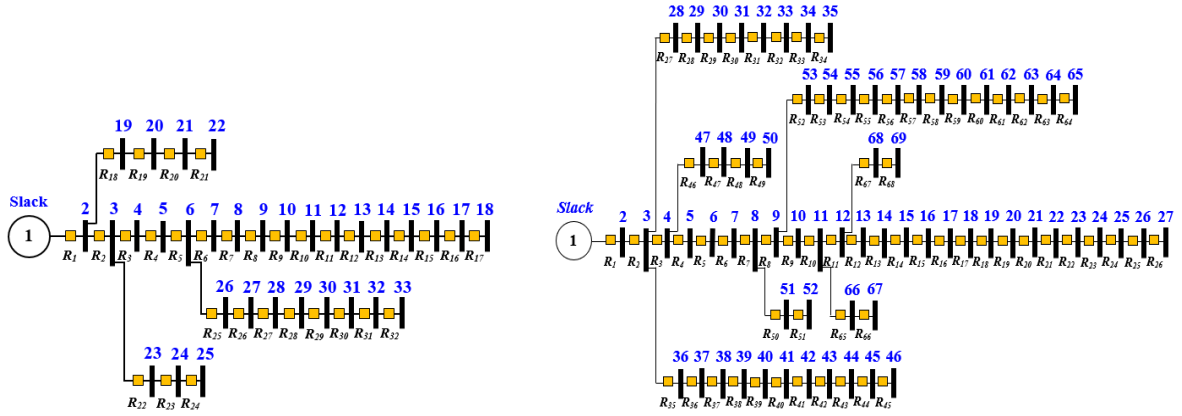


*a* *b*

Fig. 1. Single diagram of test systems: *a* – IEEE 33-bus; *b* – IEEE 69-bus

Figures 2, 3 demonstrate the curves of convergence of the applied CGWO algorithms for both cases of optimal PVDG and hybrid PVDG-BESS installation in both test systems ADNs.

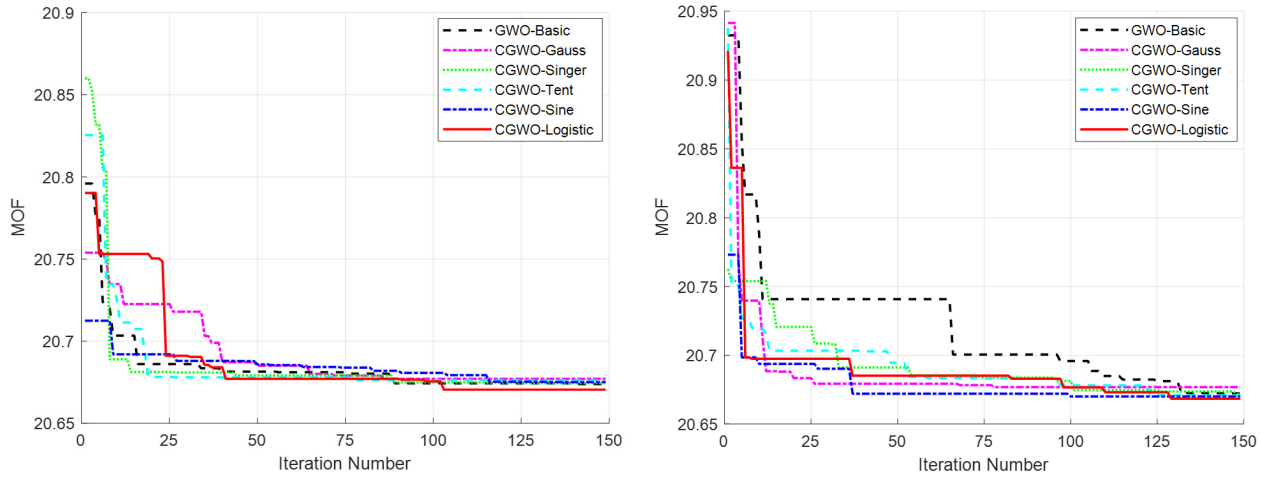


*a* *b*

Fig. 2. Convergence curves of different CGWO algorithms for the IEEE 33-bus:
*a* – PVDG; *b* – PVDG-BESS

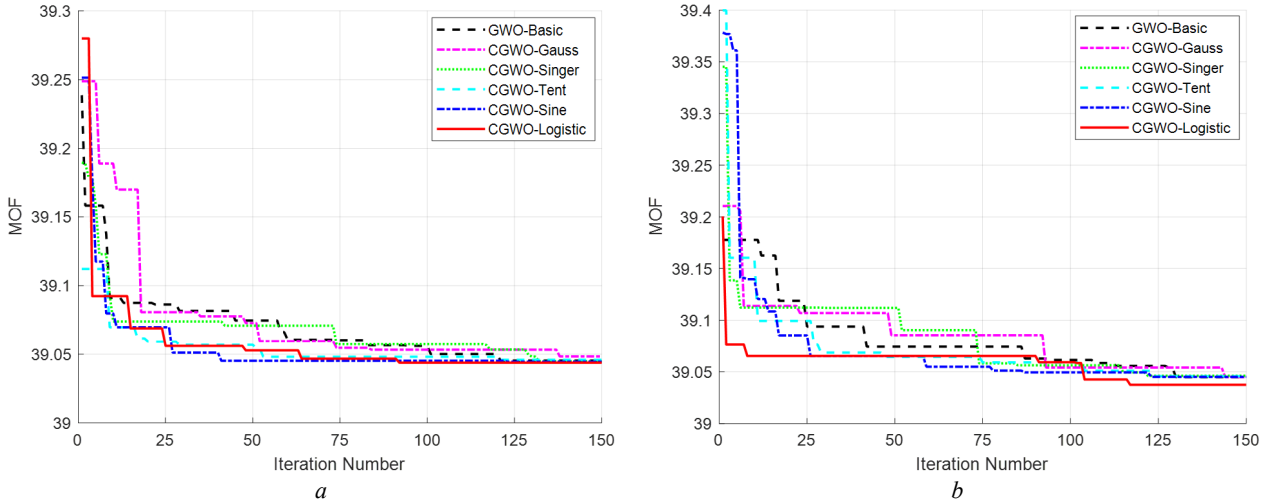


*a* *b*

Fig. 3. Convergence curves of different CGWO algorithms for the IEEE 69-bus:
*a* – PVDG; *b* – PVDG-BESS

By doing the analysis of both convergence curves, also for a maximum iterations' number equal to 150, it can be noted that the CGWO_Logistic delivered the best minimization of MOF results for both cases of PVDG and hybrid PVDG-BESS presence in both test system ADNs, comparing to the other algorithms.

For the case of only PVDG integration, the MOF got minimized by the CGWO_Logistic algorithm until 20.670 for the first test system ADN, and until 39.043 for the second system ADN.

For the case of hybrid PVDG-BESS, the MOF got minimized by the CGWO_Logistic algorithm until 20.668 for the first system, while for the second system it got minimized until 39.037, with noticing a late convergence characteristic in both cases studies for the two test systems which were in general, more than 100 iterations for all cases studies, except for the case of PVDG integration in second test system, where the CGWO_Logistic algorithm converges around 85 iterations to attain the best solution.

Figures 4, 5 illustrate the MOF boxplot results of the different applied CGWO algorithms after 20 runs in each of them, for both cases studies of optimal PVDG and hybrid PVDG-BESS integration, respectively in the two test systems ADNs.

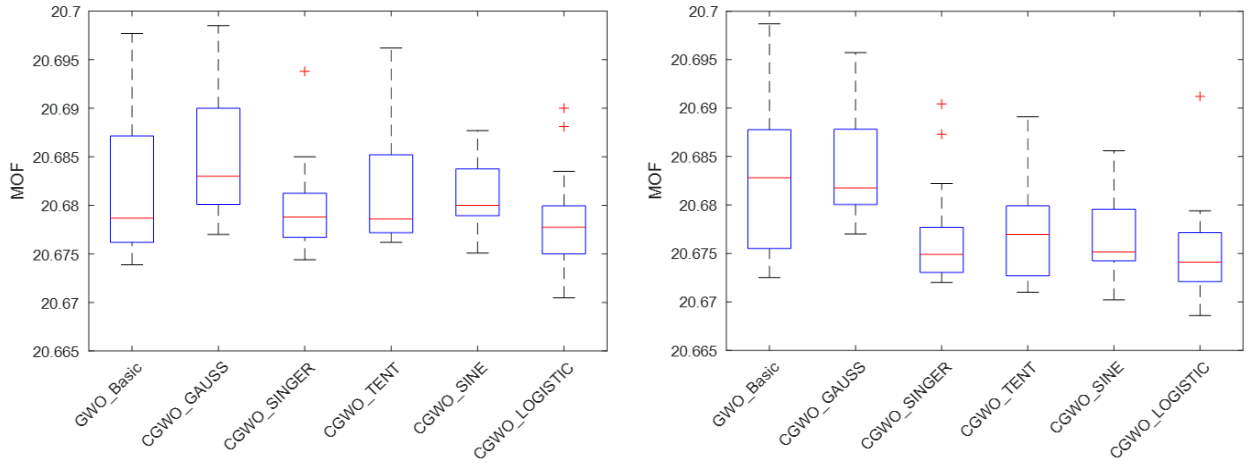


*a* *b*

Fig. 4. Boxplot of CGWO algorithms for the IEEE 33-bus:
*a* – PVDG; *b* – PVDG-BESS

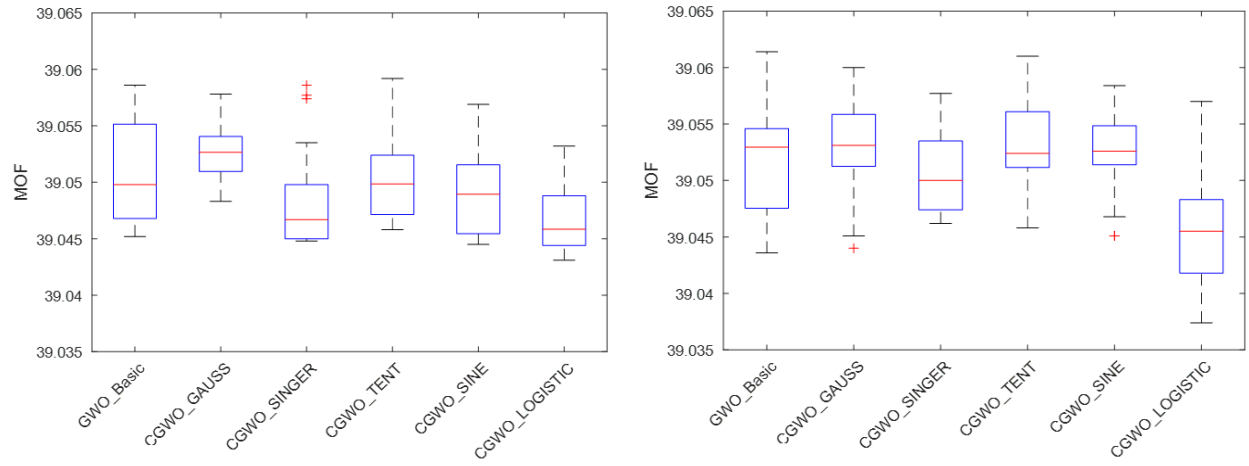


*a* *b*

Fig. 5. Boxplot of CGWO algorithms for the IEEE 69-bus:
*a* – PVDG; *b* – PVDG-BESS

For the purpose of improving the comparison and better evaluating of the utilized CGWO algorithms, a boxplot is presented as shown in Fig. 4, 5. The results were obtained while taking into account 20 runs for each applied algorithm. It can be noted for all the CGWO algorithms that the results are too close to their best and minimum MOF for all cases studies of optimal PVDG and hybrid PVDG-BESS integration in both test systems ADNs.

Besides, it is clear that the CGWO_Logistic algorithm showed efficiency and reliability when providing the lowest median and delivering the best and the minimum value of MOF in the two test systems for all cases studies.

Tables 1 and 3 show the optimal locations and sizes of both case studies (PVDG and hybrid PVDG-BESS) when applying the various CGWO algorithms on the two test systems ADNs.

Tables 2, 4 show the optimized parameters and the results obtained when optimally locate and size all cases studies (PVDG and hybrid PVDG-BESS) by various CGWO algorithms in both test systems ADNs.

From Tables 1–4 also when based on the comparison, it is clear among all the applied CGWO algorithms, that the best results and the minimum of MOF, was obtained by the CGWO_Logistic algorithm which provided the best values for the first test system ADN until 20.670 for the case of PVDG and until 20.668 for the case of hybrid PVDG-BESS. Meanwhile, for the IEEE 69-bus ADN the CGWO_Logistic algorithm provided the best MOF value of 39.043 for the case of PVDG and a value until 39.037 for the case of hybrid PVDG-BESS.

Table 1

Optimal location and sizing of all cases for the IEEE 33-bus

| Algorithms applied | Cases | Optimal buses | Sizes (kW) |
|---|---|---|---|
| GWO Basic | PVDG | 5-16-30 | 1446, 388.2, 405.4 |
| | PVDG<br>BESS | 5-14-24<br>20-21-31 | 327.8, 492.4, 1001<br>-498.1, 516.8, 570.1 |
| CGWO Gauss | PVDG | 5-15-33 | 1242, 430.7, 408.7 |
| | PVDG<br>BESS | 5-13-27<br>13-21-31 | 2091, 300.0, 458.1<br>5.7, 58.8, 477.6 |
| CGWO Singer | PVDG | 5-14-32 | 1579, 401.6, 421.8 |
| | PVDG<br>BESS | 3-5-33<br>13-21-22 | 1140, 859.9, 480.7<br>457.7, -190.7, 239.7 |
| CGWO Tent | PVDG | 4-13-32 | 1935, 470.4, 406.1 |
| | PVDG<br>BESS | 13-24-30<br>2-5-10 | 585.0, 761.7, 601.8<br>196.7, 5.5, 4.3 |
| CGWO Sine | PVDG | 5-15-33 | 1605, 392.6, 350.1 |
| | PVDG<br>BESS | 3-25-33<br>5-16-25 | 361.2, 300.0, 405.4<br>1300.3, 372.2, 319.8 |
| CGWO Logistic | PVDG | 5-16-30 | 1503, 370.4, 400.2 |
| | PVDG<br>BESS | 5-24-30<br>3-15-26 | 1346, 882.3, 488.9<br>-270, 477.5, -353.6 |

Table 2

Optimal results of all cases integration for the IEEE 33-bus

| Algorithms applied | Cases | TAPL (kW) | TVD (p.u.) | TOT (sec) | MOF |
|---|---|---|---|---|---|
| Basic Case | | 210.987 | 1.812 | 20.574 | – |
| GWO Basic | PVDG | 95.612 | 1.088 | 19.495 | 20.674 |
| | PVDG BESS | 83.020 | 1.077 | 19.516 | 20.673 |
| CGWO Gauss | PVDG | 128.474 | 1.364 | 19.257 | 20.677 |
| | PVDG BESS | 104.813 | 1.079 | 19.524 | 20.677 |
| CGWO Singer | PVDG | 92.112 | 1.062 | 19.523 | 20.674 |
| | PVDG BESS | 87.252 | 1.046 | 19.541 | 20.672 |
| CGWO Tent | PVDG | 93.014 | 1.060 | 19.525 | 20.676 |
| | PVDG BESS | 87.510 | 1.103 | 19.491 | 20.671 |
| CGWO Sine | PVDG | 124.961 | 1.318 | 19.293 | 20.675 |
| | PVDG BESS | 86.372 | 1.058 | 19.525 | 20.670 |
| CGWO Logistic | PVDG | 96.115 | 1.090 | 19.493 | 20.670 |
| | PVDG BESS | 87.397 | 1.066 | 19.521 | 20.668 |

Table 3

Optimal location and sizing of all cases for the IEEE 69-bus

| Algorithms applied | Cases | Optimal buses | Sizes (kW) |
|---|---|---|---|
| GWO Basic | PVDG | 47-63-69 | 448.8, 946.4, 389.2 |
| | PVDG<br>BESS | 4-12-61<br>13-64-68 | 1755, 581.5, 691.5<br>-143.0, 225.6, 151.0 |
| CGWO Gauss | PVDG | 4-60-69 | 1410, 1073, 459.7 |
| | PVDG<br>BESS | 5-63-69<br>3-5-62 | 670.5, 433.5, 300.0<br>272.1, -1301, 540.2 |
| CGWO Singer | PVDG | 12-38-62 | 388.8, 408.6, 974.4 |
| | PVDG<br>BESS | 14-49-61<br>4-8-56 | 315.3, 477.4, 1192<br>241.5, 69.8, -444.3 |
| CGWO Tent | PVDG | 57-61-69 | 349.4, 772.7, 381.9 |
| | PVDG<br>BESS | 12-56-69<br>2-52-61 | 453.0, 444.8, 326.9<br>-550.1, -1200, 959.6 |
| CGWO Sine | PVDG | 5-61-69 | 443.2, 982.9, 355.6 |
| | PVDG<br>BESS | 49-61-69<br>8-53-69 | 434.1, 1097, 326.9<br>2.7, -690.6, 704.7 |
| CGWO Logistic | PVDG | 4-61-69 | 707.2, 996.8, 348.9 |
| | PVDG<br>BESS | 16-50-61<br>10-36-59 | 320.5, 349.3,1256<br>-147.0, 228.8, 280.4 |

Table 4

Optimal results of all cases integration for the IEEE 69-bus

| Algorithms applied | Cases | TAPL (kW) | TVD (p.u.) | TOT (sec) | MOF |
|---|---|---|---|---|---|
| Basic case | | 224.945 | 1.870 | 38.772 | --- |
| GWO Basic | PVDG | 104.063 | 1.304 | 37.647 | 39.045 |
| | PVDG BESS | 100.870 | 1.263 | 37.690 | 39.044 |
| CGWO Gauss | PVDG | 102.901 | 1.257 | 37.697 | 39.048 |
| | PVDG BESS | 104.972 | 1.330 | 37.620 | 39.045 |
| CGWO Singer | PVDG | 101.424 | 1.296 | 37.657 | 39.045 |
| | PVDG BESS | 98.993 | 1.280 | 37.667 | 39.047 |
| CGWO Tent | PVDG | 100.252 | 1.274 | 37.681 | 39.046 |
| | PVDG BESS | 108.550 | 1.271 | 37.675 | 39.046 |
| CGWO Sine | PVDG | 101.633 | 1.304 | 37.648 | 39.045 |
| | PVDG BESS | 102.082 | 1.264 | 37.678 | 39.045 |
| CGWO Logistic | PVDG | 101.078 | 1.303 | 37.649 | 39.043 |
| | PVDG BESS | 78.497 | 1.137 | 37.821 | 39.037 |

The rest of the applied algorithms also reveal a good efficiency in delivering the best results, but in terms of each parameter on its own, where, as example for the IEEE 33-bus ADN, the CGWO_Singer algorithm delivered the minimum TAPL's value of 92.112 kW, while the CGWO_Tent algorithm delivered the minimum TVD's value of 1.060 p.u. for the case of PVDG, also the GWO_Basic algorithm delivered the minimum TAPL's value of 83.020 kW for the case of hybrid PVDG-BESS. Meanwhile, for the second test system ADN, as example, the GWO_Tent provided the minimum TAPL's value of 100.252 kW and the GWO_Basic algorithm provided the minimum TOT's value of 37.647 seconds for the case of PVDG, while the GWO_Gauss algorithm delivered the minimum TOT's value of 37.620 seconds for the case of hybrid PVDG-BESS.

Figure 6 demonstrates the comparison of active power losses between the basic case and both cases of optimal PVDG and hybrid PVDG-BESS presence in both test systems ADNs.

From Fig. 6, and the previous results, it is noted that the optimal allocation of PVDG and hybrid PVDG-BESS using the CGWO_Logistic algorithm in the two test systems, contributed excellently and directly to the minimizing of the active power losses in almost all branches of both ADNs, especially in branches which situated near to the optimally located buses of both cases integration in the two test systems, with superior and much better results for the second case study with the integration of hybrid PVDG-BESS.

Also, this comparison could be improved when basing on the TAPL value, where it is reduced at the first system IEEE 33-bus ADN, from value of 210.987 kW at the basic case to 96.115 kW for the case of PVDG, and until 87.397 kW for the case of hybrid PVDG-BESS.

For the second system ADN, the TAPL got reduced from 224.947 kW to 101.078 kW for the case of PVDG and reduced until 78.497 kW for the case of hybrid PVDG-BESS installation.

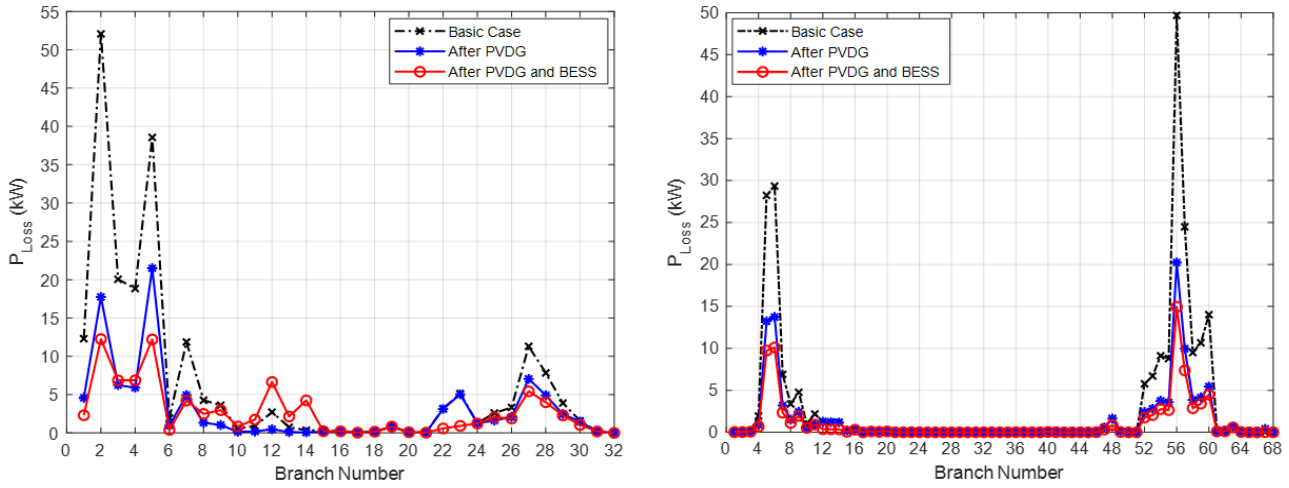


*a* *b*

Fig. 6. Active power losses in branches:
*a* – IEEE 33-bus; *b* – IEEE 69-bus

Figure 7 represents the voltage deviation for all cases studies of the optimal integration of PVDG and hybrid PVDG-BESS units in the two standards test systems ADNs.

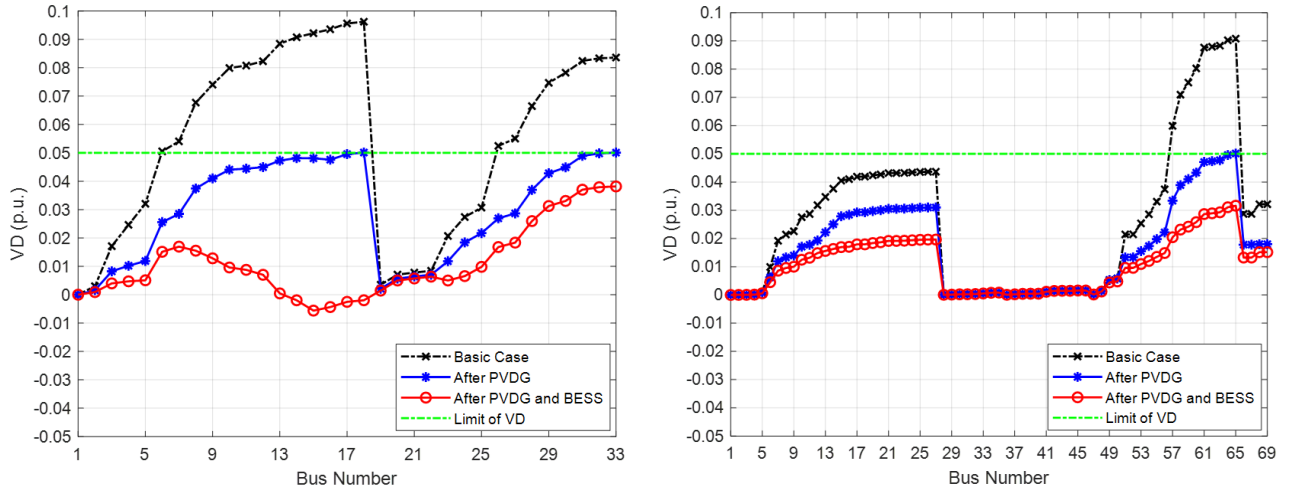


*a* *b*

Fig. 7. Bus voltage deviation:
*a* – IEEE 33-bus; *b* – IEEE 69-bus

When analyzing Fig. 7, it may be noticed that the voltage deviation at the basic case was above the limited value of 0.05 p.u. in most buses of the two test systems ADNs. Moreover, it may be observed after the optimal integration of PVDG and the hybrid PVDG-BESS into ADNs by the CGWO_Logistic algorithm, that the voltage deviation got minimized under the allowed range in all test systems' buses with superior and better results provided by the second case with the integration of hybrid PVDG-BESS systems.

Also, by checking the value of TVD, it is seen for the first system, the TVD minimized from 1.812 p.u. to 1.090 p.u. for the case of PVDG and until 1.066 p.u. for the case of hybrid PVDG-BESS. For the second system, TVD reduced from 1.870 p.u. to 1.303 p.u. for the case of PVDG and until 1.137 p.u. for the case of hybrid PVDG-BESS.

Figure 8 represents the bus voltage profiles for all cases studies of the optimal integration of PVDG and hybrid PVDG-BESS units in the two standard test systems ADNs.

From Fig. 8, it may note that the voltage profiles have improved in all buses of both standards test systems ADNs after the optimal integration of both cases studies of PVDG and hybrid PVDG-BESS units, with much better and superior results for the second case of hybrid PVDG-BESS. Also, this voltage profiles' ameliorating was especially in the buses which situated close to the optimally located buses of both cases studies integration into test systems ADNs.

As mentioned previously in Fig. 7, the minimization of the voltage deviation, consequently led to the enhancement of the voltage profiles, due to the fact that the voltage deviation is represented as the difference between the nominal voltage of 1 p.u., and the voltage value at the basic case.

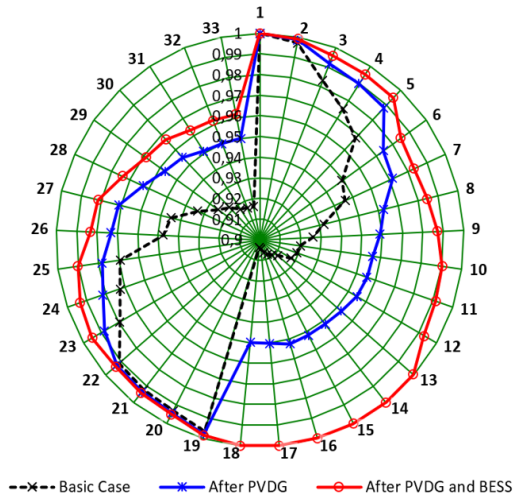


*a*

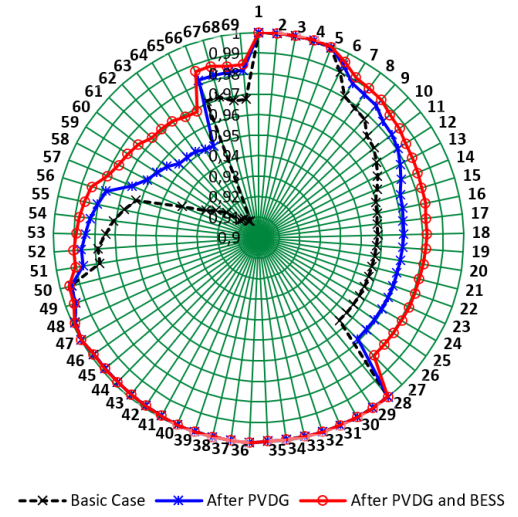


*b*

Fig. 8. Voltage profiles of buses:
*a* – IEEE 33-bus; *b* – IEEE 69-bus

Figure 9 illustrates the primary overcurrent relays' operation time with two different zones of zoom for the basic case and after all cases studies integration of PVDG and hybrid PVDG-BESS into both standards test systems ADNs.

When comparing to the basic case, it is clear that the operation time in most of the primary NS-OCRs had considerably minimized after the optimal integration of PVDG and hybrid PVDG-BESS into both test systems ADNs by the CGWO_Logistic algorithm. Besides, the TOT was decreased at the first system IEEE 33-bus ADN from 20.574 seconds to 19.493 seconds for the case of PVDG and until 19.521 seconds for the case of hybrid PVDG-BESS. Also, it is mentioned a clear impact of operation time's minimization in both zones of zoom in Fig. 9,*a*, between NS-OCRs from 12 to 14 and from 23 to 25, for both cases studies.

For the IEEE 69-bus ADN, the TOT decreased from 38.772 seconds to 37.649 seconds for the case of PVDG and until 37.821 seconds for the case of hybrid PVDG-BESS, where that impact of operation time's minimization is obvious in both zones of zoom in Fig. 9,*b* between NS-OCRs from 10 to 13 and from 50 to 54, for both cases studies. Hence, according to equation (8), this

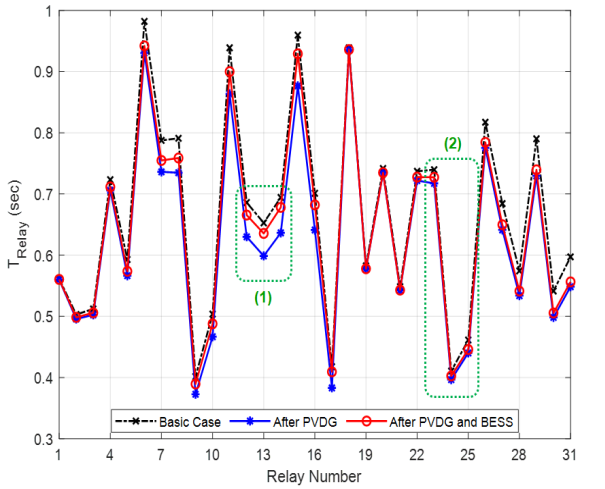


*a*

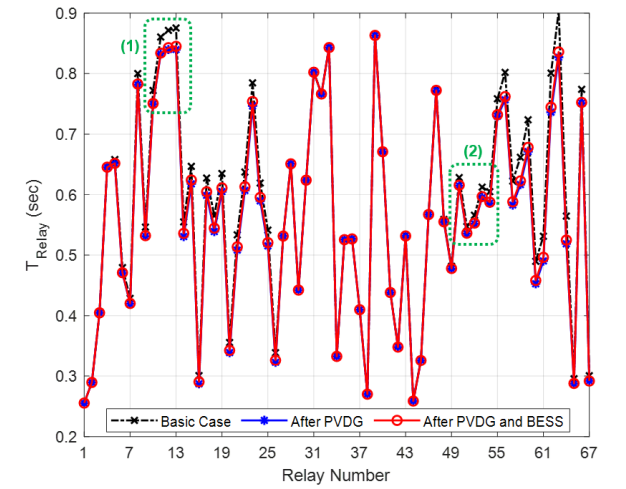


*b*

Fig. 9. Overcurrent relay operation time:
*a* – IEEE 33-bus; *b* – IEEE 69-bus

minimization was due to the inverse function between the fault current and the fault voltage magnitude covered by the NS-OCR and its operation time, where the more $I_F$ and $V_{FM}$ increased, the NS-OCR will operate quickly to clear the faults.

**5. Conclusion.**

In this paper, a study of comparison was carried out between the various chaotic grey wolf optimization

algorithms to identify the optimal allocation of multiple photovoltaic distributed generation and hybrid photovoltaic distributed generation and battery energy storage systems, into the active distribution networks based on solving the multi-objective function which represented as reducing simultaneously the three technically parameters: total voltage deviation, total active power losses and the overcurrent relays' total operation time.

The simulation results confirm the robustness and efficiency of the chaotic logistic grey wolf optimization algorithm, compared to the rest of the applied algorithms, in terms of providing the best and minimum multi-objective functions-based power losses, voltage deviation, and overcurrent relay operation time's values, but including a late convergence characteristic. The comparison between the attained results of simulation for various cases studied led toward the conclusion that best results were achieved when the photovoltaic distributed generation and battery energy storage systems were simultaneously optimally allocated, which drove to a significant minimization of power losses, ameliorating of the voltage profiles, and improvement of the overcurrent protection system in the active distribution networks studies.

Based on the previous discussion, the future work will focus on implementing the Distributed Static Var Compensator in addition to the battery energy storage systems to improve the performance of the studies systems, while considering new technical indices, also the distributed generation power outputs and the load demand variation at the different sessions of the year.

**Conflict of interest.** The authors declare that they have no conflicts of interest.

REFERENCES


***1.*** Lai C.S., Jia Y., Lai L.L. A comprehensive review on large-scale photovoltaic system with applications of electrical energy storage. *Renewable and Sustainable Energy Reviews*, 2017, vol. 78, pp. 439-451. doi: https://doi.org/10.1016/j.rser.2017.04.078.

***2.*** Wong L.A., Ramachandaramurthy V.K., Taylor P., Ekanayake J.B., Walker S.L., Padmanaban S. Review on the optimal placement, sizing and control of an energy storage system in the distribution network. *Journal of Energy Storage*, 2019, vol. 21, pp. 489-504. doi: https://doi.org/10.1016/j.est.2018.12.015.

***3.*** Macedo L.H., Franco J.F., Rider M.J., Romero R. Optimal operation of distribution networks considering energy storage devices. *IEEE Transactions on Smart Grid*, 2015, vol. 6, no. 6, pp. 2825-2836. doi: https://doi.org/10.1109/tsg.2015.2419134.

***4.*** Hemmati R. Mobile model for distributed generations and battery energy storage systems in radial grids. *Journal of Renewable and Sustainable Energy*, 2019, vol. 11, no. 2, p. 025301. doi: https://doi.org/10.1063/1.5079698.

***5.*** Home-Ortiz J.M., Pourakbari-Kasmaei M., Lehtonen M., Sanches Mantovani J.R. Optimal location-allocation of storage devices and renewable-based DG in distribution systems. *Electric Power Systems Research*, 2019, vol. 172, pp. 11-21. doi: https://doi.org/10.1016/j.epsr.2019.02.013.

***6.*** Santos S.F., Fitiwi D.Z., Cruz M.R.M., Cabrita C.M.P., Catalão J.P.S. Impacts of optimal energy storage deployment and network reconfiguration on renewable integration level in distribution systems. *Applied Energy*, 2017, vol. 185, pp. 44-55. doi: https://doi.org/10.1016/j.apenergy.2016.10.053.

***7.*** Zafar R., Ravishankar J., Fletcher J.E., Pota H.R. Multi-timescale model predictive control of battery energy storage system using conic relaxation in smart distribution grids. *IEEE Transactions on Power Systems*, 2018, vol. 33, no. 6, pp. 7152-7161. doi: https://doi.org/10.1109/tpwrs.2018.2847400.

***8.*** Bai L., Jiang T., Li F., Chen H., Li X. Distributed energy storage planning in soft open point based active distribution networks incorporating network reconfiguration and DG reactive power capability. *Applied Energy*, 2018, vol. 210, pp. 1082-1091. doi: https://doi.org/10.1016/j.apenergy.2017.07.004.

***9.*** Lei J., Gong Q. Operating strategy and optimal allocation of large-scale VRB energy storage system in active distribution networks for solar/wind power applications. *IET Generation, Transmission & Distribution*, 2017, vol. 11, no. 9, pp. 2403-2411. doi: https://doi.org/10.1049/iet-gtd.2016.2076.

***10.*** Alharthi H., Alzahrani A., Shafiq S., Khalid M. Optimal allocation of batteries to facilitate high solar photovoltaic penetration. *9th International Conference on Power and Energy Systems (ICPES 2019),* Perth, Australia, 2019. doi: https://doi.org/10.1109/icpes47639.2019.9105479.

***11.*** Ahmed H.M.A., Awad A.S.A., Ahmed M.H., Salama M.M.A. Mitigating voltage-sag and voltage-deviation problems in distribution networks using battery energy storage systems. *Electric Power Systems Research*, 2020, vol. 184, art. no. 106294. doi: https://doi.org/10.1016/j.epsr.2020.106294.

***12.*** Sardi J., Mithulananthan N., Gallagher M., Hung D.Q. Multiple community energy storage planning in distribution networks using a cost-benefit analysis. *Applied Energy*, 2017, vol. 190, pp. 453-463. doi: https://doi.org/10.1016/j.apenergy.2016.12.144.

***13.*** Zheng Y., Hill D.J., Dong Z.Y. Multi-agent optimal allocation of energy storage systems in distribution systems. *IEEE Transactions on Sustainable Energy,* 2017, vol. 8, no. 4, pp. 1715-1725. doi: https://doi.org/10.1109/tste.2017.2705838.

***14.*** Zhang Y., Xu Y., Yang H., Dong Z.Y. Voltage regulation-oriented co-planning of distributed generation and battery storage in active distribution networks. *International Journal of Electrical Power and Energy Systems*, 2019, vol. 105, pp. 79-88. doi: https://doi.org/10.1016/j.ijepes.2018.07.036.

***15.*** Gao J., Chen J.-J., Cai Y., Zeng S.-Q., Peng K. A two-stage Microgrid cost optimization considering distribution network loss and voltage deviation. *Energy Reports*, 2020, vol. 6, no. 2, pp. 263-267. doi: https://doi.org/10.1016/j.egyr.2019.11.072.

***16.*** Luo L., Abdulkareem S.S., Rezvani A., Miveh M.R., Samad S., Aljojo N., Pazhoohesh M. Optimal scheduling of a renewable based microgrid considering photovoltaic system and battery energy storage under uncertainty. *Journal of Energy Storage*, 2020, vol. 28, art. no. 101306. doi: https://doi.org/10.1016/j.est.2020.101306.

***17.*** Chen J., Jiang X., Li J., Wu Q., Zhang Y., Song G., Lin D. Multi-stage dynamic optimal allocation for battery energy storage system in distribution networks with photovoltaic system. *International Transactions on Electrical Energy Systems*, 2020, vol. 30, no. 12, art. no. e12644. doi: https://doi.org/10.1002/2050-7038.12644.

***18.*** Khalid M., Akram U., Shafiq S. Optimal planning of multiple distributed generating units and storage in active distribution networks. *IEEE Access*, 2018, vol. 6, pp. 55234-55244. doi: https://doi.org/10.1109/access.2018.2872788.

***19.*** Wong L.A., Ramachandaramurthy V.K., Walker S.L., Taylor P., Sanjari M.J. Optimal placement and sizing of battery energy storage system for losses reduction using whale optimization algorithm. *Journal of Energy Storage*, 2019, vol. 26, art. no. 100892. doi: https://doi.org/10.1016/j.est.2019.100892.

***20.*** Mukhopadhyay B., Das D. Multi-objective dynamic and static reconfiguration with optimized allocation of PV-DG and battery energy storage system. *Renewable and Sustainable Energy Reviews*, 2020, vol. 124, art. no. 109777. doi: https://doi.org/10.1016/j.rser.2020.109777.

***21.*** Qian X., Zhang S., Liu J., Zheng Y., Liu W. Hierarchical optimal planning of battery energy storage systems in radial distribution networks. *3rd IEEE Conference on Energy Internet*

*and Energy System Integration (EI2 2019)*, Changsha, China 2019. doi: https://doi.org/10.1109/EI247390.2019.9061757.
***22.*** Ahmadi B., Ceylan O., Ozdemir A. Voltage profile improving and peak shaving using multi-type distributed generators and battery energy storage systems in distribution networks. *55th International Universities Power Engineering Conference (UPEC 2020)*, Italy, 2020. doi: https://doi.org/10.1109/upec49904.2020.9209880.
***23.*** Valencia A., Hincapie R.A., Gallego R.A. Optimal location, selection, and operation of battery energy storage systems and renewable distributed generation in medium–low voltage distribution networks. *Journal of Energy Storage*, 2021, vol. 34, art. no. 102158. doi: https://doi.org/10.1016/j.est.2020.102158.
***24.*** Mirjalili S., Mirjalili S.M., Lewis A. Grey wolf optimizer. *Advances in Engineering Software*, 2014, vol. 69, pp. 46-61. doi: https://doi.org/10.1016/j.advengsoft.2013.12.007.
***25.*** Lu C., Gao L., Li X., Hu C., Yan X., Gong W. Chaotic-based grey wolf optimizer for numerical and engineering optimization problems. *Memetic Computing*, 2020, vol. 12, no. 4, pp. 371-398. doi: https://doi.org/10.1007/s12293-020-00313-6.
***26.*** Settoul S., Chenni R., Hassan H.A., Zellagui M., Kraimia M.N. MFO Algorithm for optimal location and sizing of multiple photovoltaic distributed generations units for loss reduction in distribution systems. *7th International Renewable and Sustainable Energy Conference (IRSEC 2019)*. Morocco, 2019. doi: https://doi.org/10.1109/irsec48032.2019.9078241.
***27.*** Zellagui M., Settoul S., Lasmari A., El-Bayeh C.Z., Chenni R., Hassan H.A. Optimal allocation of renewable energy source integrated-smart distribution systems based on technical-economic analysis considering load demand and DG uncertainties. *Lecture Notes in Networks and Systems*. 2021, vol. 174, pp. 391-404. doi: https://doi.org/10.1007/978-3-030-63846-7_37.
***28.*** Belbachir N., Zellagui M., Lasmari A., El-Bayeh C.Z., Bekkouche B. Optimal PV sources integration in distribution system and its impacts on overcurrent relay based time-current-voltage tripping characteristic. *12th International Symposium on Advanced Topics in Electrical Engineering (ATEE 2021),* Romania, 2021. doi: https://doi.org/10.1109/atee52255.2021.9425155.
***29.*** Lasmari A., Zellagui M., Hassan H.A., Settoul S., Abdelaziz A.Y., Chenni R. Optimal energy-efficient integration of photovoltaic DG in radial distribution systems for various load models. *11th International Renewable Energy Congress, (IREC 2020),* Tunisia, 2020. doi: https://doi.org/10.1109/irec48820.2020.9310429.
***30.*** Saleh K.A., Zeineldin H.H., Al-Hinai A., El-Saadany E.F. Optimal coordination of directional overcurrent relays using a new time-current-voltage characteristic. *IEEE Transactions on Power Delivery.* 2015, vol. 30, pp. 537-544. doi: https://doi.org/10.1109/TPWRD.2014.2341666.
***31.*** Saremi S., Mirjalili S.Z., Mirjalili S.M. Evolutionary population dynamics and grey wolf optimizer. *Neural Computing and Applications*, 2015, vol. 26, no. 5, pp. 1257-1263. doi: https://doi.org/10.1007/s00521-014-1806-7.
***32.*** Saremi S., Mirjalili S., Lewis A. Biogeography-based optimization with chaos. *Neural Computing and Applications*, 2014, vol. 25, no. 5, pp. 1077-1097. doi: https://doi.org/10.1007/s00521-014-1597-x.

*Received 12.05.2021*
*Accepted 14.06.2021*
*Published 25.06.2021*

*Nasreddine Belbachir*[1], *PhD Student,*
*Mohamed Zellagui*[2], *PhD, Associate Professor,*
*Samir Settoul*[3], *PhD Student,*
*Claude Ziad El-Bayeh*[4], *PhD, Postdoctoral Research,*
*Benaissa Bekkouche*[1], *PhD, Professor,*
[1] Department of Electrical Engineering,
University of Mostaganem, Mostaganem, 27000, Algeria,
e-mail: n.belbachir@ieee.org (Corresponding author),
benaissa.bekkouche@univ-mosta.dz
[2] Department of Electrical Engineering,
University of Batna 2, Fesdis, Batna, 05078, Algeria,
e-mail: m.zellagui@ieee.org, m.zellagui@univ-batna2.dz
[3] Department of Electrotechnic,
Mentouri University of Constantine 1,
Constantine, 25000, Algeria,
e-mail: samir.settoul@umc.edu.dz
[4] Canada Excellence Research Chairs Team,
Concordia University,
Montreal, Quebec, H3G 1M8, Canada,
e-mail: c.bayeh@hotmail.com